# Electron Paramagnetic Resonance Stopped-Flow Kinetic Study of Manganese(II) Sorption–Desorption on Birnessite

S. E. Fendorf,* D. L. Sparks, J. A. Franz, and D. M. Camaioni

## ABSTRACT

**Many important reactions involving colloidal suspensions are rapid. Here, we introduce the application of a technique capable of rapidly measuring a reactant species (within 20 ms after the reaction initiation) in situ: an electron paramagnetic resonance spectroscopically monitored stopped-flow method (EPR–SF). The utility of this technique is demonstrated by investigating the sorption of $Mn^{2+}$ on $\delta$-$MnO_2$. The sorption reaction was complete in <1 s, with >80% of the $Mn^{2+}$ being sorbed within 200 ms. A first-order rate dependence on $Mn^{2+}$ was observed. Measurement of the initial reaction rate allowed the forward (sorption) rate constant to be determined ($k_f$ = 3.74 × $10^{-3}$ $s^{-1}$), and the reverse (desorption) rate constant was determined using an integrated reversible first-order rate expression ($k_r$ = 3.08 × $10^{-4}$ $s^{-1}$). Using these rate constants, the predicted time dependence of $Mn^{2+}$ sorption was in good agreement with the measured sorption rate. The results indicate that chemical kinetics are being measured that allow determination of precise reaction rates and mechanisms.**

DETERMINING REACTION RATES and mechanisms is essential for understanding chemical processes (Sparks, 1989). Advances in methodologies have allowed investigation of many rapid reactions in gas, solution, and solid phases. Few methods exist, however, for measurement of rapid reactions of colloidal suspensions. Many techniques that are currently used to study colloidal suspensions measure both physical (i.e., transport or diffusion) and chemical phenomena simultaneously, which greatly complicates the measurement of elementary reactions or rate-controlling processes. Moreover, apparent rate laws and parameters are measured. Measuring chemical kinetics allows one to ascertain reaction rates and mechanisms, knowledge of which is necessary to understand, predict, and control reaction pathways. Reactions of colloidal suspensions are of interest to scientists in an array of fields: catalysis, electrochemistry, and environmental and soil chemistry. Therefore, it is important to develop methods that are capable of measuring chemical kinetics in such systems. In this study, we demonstrate the application of an EPR–SF kinetic technique that, for an EPR-active metal species, enables the rapid and direct in situ detection of reactions in a colloidal suspension.

To obtain chemical kinetic information, a technique must be able to monitor a reaction during the time frame in which it occurs while minimizing the effects of diffusion on the reaction rate. However, many soil chemical processes are rapid, precluding the use of traditional batch or flow techniques (Sparks, 1989). Filtration of suspensions prior to analysis has been extensively used to monitor the solution components of suspensions, but the time for filtration itself often limits the study of rapid reactions. Chemical relaxation techniques have been used to investigate suspension reactions by monitoring a system parameter related to a species concentration (e.g., electrical conductivity) that is not adversely affected by the presence of colloidal material (Ikeda et al., 1983, 1984; Hayes and Leckie, 1986; Zhang and Sparks, 1990). With many of these techniques, however, the reaction must be fully reversible, reactant species are not directly measured, and rate constants are determined from linearized rate equations that often are dependent on equilibrium parameters. Since the stopped-flow mixing can be carried out ≤20 ms (and EPR signal digitized within a few microseconds), the EPR–SF technique eliminates the conventional limitations of measuring colloidal reactions, allowing rapid direct measurement of a reactant species in situ.

Stopped-flow kinetic methods have found limited use in colloidal chemistry (Ikeda et al., 1984). These methods, however, have been employed to study biochemical reactions, and EPR spectroscopically measured stopped flow kinetics has been applied to the study of biological solution chemistry (Klimes et al., 1980; Stach et al., 1985). Klimes et al. (1980) found that the time-limiting factor in EPR–SF was the mixing rate of the stopped-flow cell. The time resolution of stopped-flow mixing is generally <20 ms with mix-

S.E. Fendorf and D.L. Sparks, Dep. of Plant and Soil Sciences, Univ. of Delaware, Newark, DE 19717-1303; and J.A. Franz and D.M. Camaioni, Pacific Northwest Lab., P.O. Box 999, Richland, WA 99352. Received 2 Dec. 1991. *Corresponding author.

Published in Soil Sci. Soc. Am. J. 57:57–62 (1993).

**Abbreviations:** EPR–SF, electron paramagnetic resonance spectroscopically monitored stopped-flow method; ZPC, zero point of charge.

ing efficiency of 90% or greater (Klimes et al., 1980; Ikeda et al., 1984), and has been reduced to 1 ms for an electromagnetically driven accelerated-flow system (Stach et al., 1985). Therefore, EPR–SF is capable of monitoring reactions with a half-life >20 ms.

The EPR–SF technique offers many advantages for studying sorption reactions that have an EPR-detectable constituent of interest. Many organic molecules (especially free radicals), in addition to $Mn^{2+}$ and $Cu^{2+}$, are EPR active and of interest to soil and environmental scientists; a host of other constituents are EPR active and of possible interest in other chemical fields. For an EPR-active (paramagnetic) species, the unpaired electron spin moment interacts with a magnetic field, which gives rise to different energy states; this in turn allows energy in the microwave frequency to be absorbed by the species, which can then be measured (Drago, 1977). A species that is EPR active in solution often may not be EPR active when it is in a sorbed state due to rapid spin relaxation pathways, or the spectra may be broadened to the point where they contribute insignificantly to the signal intensity (McBride, 1982; Bleam and McBride, 1986). Consequently, the sorption of an EPR-active species can be monitored by the reduction in signal intensity, which allows one to determine sorption kinetics. In addition, desorption kinetics can also be measured by monitoring the signal intensity after a sudden decrease in the sorptive concentration of the suspension (i.e., after the solution concentration undergoes a perturbation and is decreased, the system readjusts to the new equilibrium by desorbing surface-bound species, which can thus be measured as a function of time). Electron paramagnetic resonance spectroscopy has been extensively used to investigate sorption and oxidation reactions on soil constituents (Clementz et al., 1973; McBride, 1982, 1987, 1989; Bleam and McBride, 1986). However, EPR has not been applied to kinetic investigations of colloidal materials.

The binding of solution species to solid surfaces present in soil and water systems is a primary determinant in the behavior of many substances. Such processes can tie up plant nutrients, remove hazardous contaminants, and modify mineral surfaces. Manganese$^{2+}$ is a model EPR-active species; hence, for reactions in which this ion is involved, EPR–SF kinetics is ideal. The intent of this study was to develop a stopped-flow kinetic technique monitored by EPR spectroscopy that could directly measure rapid reaction rates. Here, we used $Mn^{2+}$ sorption on $\delta$-$MnO_2$ to demonstrate the utility of this technique for the study of colloidal reactions, but this technique is suitable for any EPR-active species. In addition to monitoring sorption–desorption reactions, this technique is also capable of measuring redox reactions involving Mn oxides, as $Mn^{2+}$ is liberated during such processes. We are currently using this technique to investigate reactions of this type.

## MATERIALS AND METHODS

A schematic diagram of the instrumental setup is shown in Fig. 1. Dual 2-mL in-port syringes feed an EPR–SF mixing cell (Hi-Tech Scientific Ltd., Salisbury, England). The mixing cell (Model wg-385-b, Wilmad Glass Co., Buena, NJ, a variable-temperature aqueous mixing cell) is located in the EPR spectrometer, allowing EPR detection of the cell contents. A single outflow port is fitted with a 2-mL effluent collection syringe equipped with a triggering switch. The triggering switch activates the data acquisition system (Microstar Electronics, Redmind, WA, Model DAP 2400 data acquisition processor board mounted in an IBM Model AT). Each run consists of filling the in-port syringes with the desired reactants, flushing the system with the reactants several times, and finally initiating and monitoring the reaction. Consecutive runs can be conducted with the same reactants simply by repeating this procedure.

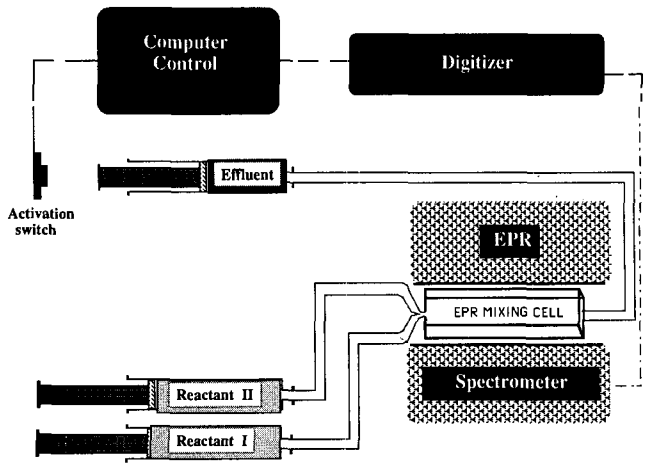


**Fig. 1 Schematic diagram of the electron paramagnetic resonance monitored stopped-flow kinetic apparatus.**

To obtain quantitative information on $Mn^{2+}$, the EPR cell was filled with a known concentration of $Mn^{2+}$ (in the absence of colloidal material). The magnetic field was then swept, resulting in the $Mn^{2+}$ hyperfine sextet structure (inset in Fig. 2). The magnetic field was centered at the down-field peak for quantitative measurement of the $Mn^{2+}$ present in solution. Known solution concentrations of $Mn^{2+}$ were used to relate the EPR signal with the $Mn^{2+}$ concentration. Figure 2 shows the linear relationship between the EPR signal and $Mn^{2+}$ concentration within the range of 5 to 500 $\mu M$ $Mn^{2+}$.

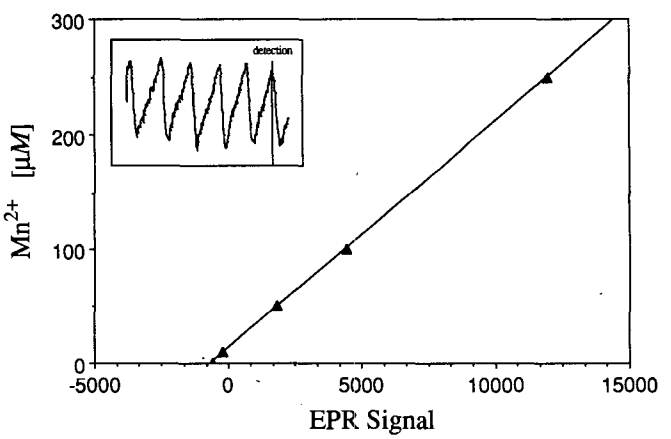


**Fig. 2. The standard curve relating the electron paramagnetic resonance signal intensity of the down-field hyperfine peak to solution $Mn^{2+}$ concentration. An excellent linear relation was consistently obtained between signal intensity and $Mn^{2+}$ concentration — the correlation coefficient was never less than one to three significant digits. Inset: the sextet hyperfine structure of $Mn^{2+}_{aqueous}$.**

For the sorption reaction, we used 50 or 80 $\mu M$ $Mn^{2+}$ in reactant syringe 1, and 1 g/L $MnO_2$ (synthetic birnessite) in reactant syringe 2. The $Mn^{2+}$ solutions were made from their $NO_3$ salts with $N_2$(g)-saturated deionized water. The properties of the oxide are given elsewhere (Fendorf and Zasoski, 1991). Equal volumes from each syringe are injected into the mixing cell, yielding initial reactant concentrations of 25 and 40 $\mu M$ $Mn^{2+}$ and 0.5 g/L $MnO_2$. At least four runs were signal averaged to yield the final data presented in this research. The reactions were carried out at pH = 5.0 in 0.001 $M$ $NaNO_3$, and pH was maintained constant with a 0.001 $M$ acetate buffer (experimental runs were conducted with and without the acetate buffer and did not differ appreciably). The particle size of the oxide was $<2\mu m$ and a stable suspension was formed at this ionic strength for times well exceeding the experimental run time.

## RESULTS AND DISCUSSION

Chemical kinetics gives mechanistic information about a reaction by allowing one to hypothesize a reaction mechanism that can be tested with experimental data. At pH = 5, the following complexation reaction of $Mn^{2+}$ on $\delta$-$MnO_2$ is suggested for low $Mn^{2+}$ surface loadings:

$$[Mn^{2+}] + S- \underset{k_r}{\overset{k_f}{\rightleftharpoons}} S\text{–}Mn + H^+ \qquad [1]$$

Where, $[Mn^{2+}]$ is the solution concentration of $Mn^{2+}$, $S-$ is the surface site, $S$–Mn is the complexed (sorbed) $Mn^{2+}$, $k_f$ is the forward (sorption) rate constant, and $k_r$ is the reverse (desorption) rate constant. Recently, Hiemstra et al. (1989a,b) have used surface structural crystallographic considerations to determine proton affinities of oxides. Three primary surface site types were evaluated, of which the O(H) surface group is either singly, doubly, or triply coordinated by the central cation of the oxide. The proton affinities of these sites are dramatically different due to their differing coordination environments. For $MnO_2$, in which Mn (the central cation) is coordinated by six O, two surface types are reactive under normal pH ranges: singly coordinated O(H) and doubly coordinated O(H) groups. At pH = 5, based on the ZPC of this oxide (ZPC = 2.8; Fendorf and Zasoski, 1992) and known proton affinities (Balistrieri and Murray, 1982; Hiemstra et al., 1989b), the singly coordinated groups are protonated and the doubly coordinated groups are deprotonated (oxo), as depicted in the following protonation reactions:

$$Mn\text{–}OH_2^{+2/3} \rightleftharpoons Mn\text{–}OH^{-1/3} + H^+ \qquad pK \approx 3.3 \qquad [2]$$

$$Mn_2\text{–}OH^{+1/3} \rightleftharpoons Mn_2\text{–}OH^{-2/3} + H^+ \qquad pK \approx 2.3 \qquad [3]$$

where $pK$ is the negative log of the dissociation constant $K$ (i.e., at pH = 5, the surface species on the product side of Eq. [2] and [3] would predominate, $Mn\text{–}OH^{-1/3}$ and $Mn_2\text{–}O^{-2/3}$). On the dominant (010) surface plane of $\delta$–$MnO_2$, these two types of sites are adjacent to one another (Arrhenius et al., 1979; Potter and Rossman, 1979). Therefore, at pH 5, bidentate complexation of $Mn^{2+}$ (Balistrieri and Murray, 1982; Morgan and Stumm, 1964) would displace one proton — in agreement with empirical observations (Morgan and Stumm, 1964). Figure 3 illustrates the surface structure of the (010) plane and the hypothesized $Mn^{2+}$ complexation reactions. At higher pH values (pH > 6.4), more than one proton is released for each $Mn^{2+}$ sorbed. The increased proton release can be explained by a polymerization of $Mn^{2+}$–hydroxide, which would form surface clusters similar to those observed on $TiO_2$ (Bleam and McBride, 1986). Under the reaction conditions employed in this study, however, cluster formation would not be expected. Charge balance in this system would be maintained by the back-

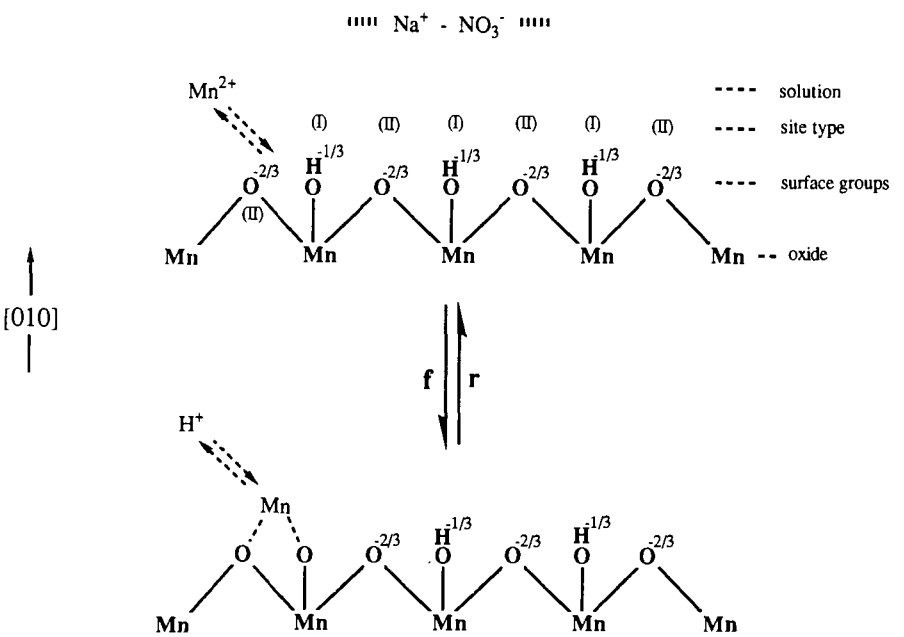


**Fig. 3. A depiction of the (010) surface plane of $\delta$-$MnO_2$ with the surface functional groups represented at pH = 5. Singly (site Type I)and doubly (site Type II) coordinated O(H) groups are shown, which are present adjacent to each other, along with the bidentate complexation of $Mn^{2+}$.**

ground electrolyte ($Na^+$ and $NO_3^-$), which were maintained in large excess to simplify reaction conditions. Hence, in our representation, *S*– would represent these two functional groups as a single site and charge balance would be maintained by the unrepresented background electrolyte.

In the overall sorption reaction, one proton is thus released for each $Mn^{2+}$ sorbed at pH 5 after steady-state conditions have been reached (Morgan and Stumm, 1964). The forward (sorption) reaction would thus not be influenced by $H^+$, provided the surface functional groups are not altered. By maintaining a constant pH, the $H^+$ term in the reverse (desorption) rate expression can be incorporated into the reaction coefficient. This was the case in our experiments. In addition, the release of surface $H^+$ is often considered to be a slow structural rearrangement of the solid phase (Dzombak and Morel, 1990), and thus would not enter into the rapid sorption mechanism investigated in this research. Furthermore, the reaction rate was not influenced by further increases in solution pH to pH = 6. Thus, the forward reaction should be dependent on $[Mn^{2+}]$ and [*S*–]; being first order in $[Mn^{2+}]$ and [*S*–], and second order overall if it is an elementary reaction. The reverse reaction would be dependent on the amount of $Mn^{2+}$ complexed, [*S*–Mn], and $[H^+]$.

Reaction [1] is of the type $A + B \rightleftharpoons C + D$, and leads to the following second-order reversible rate expression:

$$d[Mn^{2+}]/dt = -k_f[Mn^{2+}][S-] + k_r[S\text{–}Mn][H^+] \quad [4]$$

where *t* is time. By ensuring a large excess of sorbent over sorptive ($[S-] \gg [Mn^{2+}]$), and maintaining a constant pH, however, the overall reaction should be pseudo first order, depending only on $[Mn^{2+}]$. Thus, under the reaction parameters employed in this study, the rate expression would be simplified to a pseudo-first-order reaction.

$$d[Mn^{2+}]/dt = -k_f'[Mn^{2+}] + k_r'[S\text{–}Mn] \quad [5]$$

where $k_f' = k_f[S-]$ and $k_r' = k_r[H^+]$. Integration of the above simplified reversible first-order rate expression (Eq. [5]) leads to:

$$\ln\{[1 + (k_r'/k_f')]([Mn^{2+}]/[Mn^{2+}]_o) - (k_r'/k_f')\} = -(k_f' + k_r')t \quad [6]$$

Unfortunately, $k_f'$ and $k_r'$ cannot be independently determined solely from rate information on the sorption of $Mn^{2+}$ (one equation, two unknowns) without a further simplifying assumption. If one assumes that at the onset of the reaction the initial reaction rate will be dominated by the forward reaction, and the initial reaction rate can be accurately measured, then the forward rate constant can be ascertained using a first-order nonreversible analysis (in which $k_f'$ can be determined from the time-dependent $Mn^{2+}$ sorption data). The reverse reaction rate constant, $k_r'$ can then be calculated using $k_f'$ and the integrated expression for a reversible first-order reaction (Eq. [6]).

The following discussion uses this approach to determine the forward and reverse rate constants for $Mn^{2+}$ sorption on $\delta$-$MnO_2$. With a knowledge of $k_f'$ and $k_r'$, a rearrangement of Eq. [6] allows one to calculate the $Mn^{2+}$ sorption as a function of time. Thus, once the rate constants are determined, the validity of the above approach can be verified by predicting the time dependence of $Mn^{2+}$ sorption and comparing the predicted trends with those that are measured.

Because the forward rate is much greater at the onset of the reaction, measuring initial reaction rates should allow one to measure only the forward (sorption) rate constant, $k_f$. For the system parameters defined previously and a site density of 12 sites/nm$^2$ (Morgan and Stumm, 1964), the number of sorption sites would be at least two orders of magnitude greater (>100×) than the number of $Mn^{2+}$ ions present, even at the highest $Mn^{2+}$ concentration.

The following reaction is hypothesized to represent the contributing species of reaction [1] for the sorption of $Mn^{2+}$ by $MnO_2$ (i.e., for the initial reaction rate and conditions employed in this study):

$$Mn^{2+} \rightarrow S\text{–}Mn \quad [7]$$

Reaction [7] is valid far from equilibrium where $R_{sorption} \gg R_{desorption}$ (where *R* is the reaction rate, $d[Mn^{2+}]/dt$); thus, $k_f[Mn^{2+}] - k_r[Mn\text{–}S] \approx k_f[Mn^{2+}]$. The rate dependence can be described as

$$R = d[Mn^{2+}]/dt = k_f'[Mn^{2+}] \quad [8]$$

The first-order dependence of $[Mn^{2+}]$ can be evaluated using the integrated form of Eq. [8] (Sparks, 1989):

$$\log[Mn^{2+}]_t = \log[Mn^{2+}]_o - \frac{kt}{2.303} \quad [9]$$

Under pseudo-first-order conditions for $[Mn^{2+}]$, the time dependence of $[Mn^{2+}]$ is thus given by Eq. [9]. Therefore, if the reaction is assumed to be nonreversible (which should be the case at the onset of the sorption reaction) and first order in $[Mn^{2+}]$, a semilog plot of $[Mn]_t$ vs. *t* should result in a straight line with the slope = $k/2.303$, and $\log [Mn^{2+}]_0$ being the intercept.

Obtaining a linear plot based on Eq. [9], however, is necessary but not definitive proof that the reaction is first order (Sparks, 1989). If the reaction is truly first order, the rate constant should not vary with the concentration of $Mn^{2+}$. This provides a good test for a proposed reaction order; if the reaction is first-order, the slope of the semilog plot should remain unchanged with varying $[Mn^{2+}]$.

In order to deduce mechanistic information on the sorption of $Mn^{2+}$ on $\delta$-$MnO_2$ and to confirm the reaction order, two initial concentrations of $Mn^{2+}$ were used, 40 and 25 $\mu M$. Figure 4 illustrates the typically observed decay of solution $Mn^{2+}$ as a function of time. Here, data were taken every 50$\mu$s and 100 points were averaged to give the time-dependent sorption of $Mn^{2+}$ as shown (Fig. 4). Although not shown, >80% of the sorption reactions were complete for both initial $Mn^{2+}$ concentration within 200 ms.

If Eq. [7] is correct and elementary, a linear semilog plot of $[Mn^{2+}]$ as a function of time should result that is independent of $[Mn^{2+}]$ (Fig. 5). The correlation coeffi-

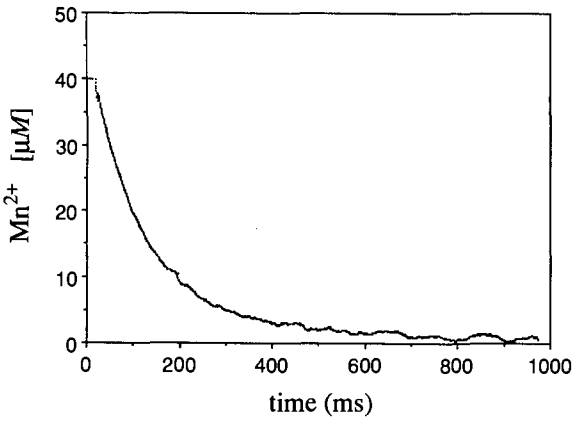


**Fig. 4. A typical rate curve of $Mn^{2+}$ sorption on $\delta$-$MnO_2$ (40 $\mu M$ initial $Mn^{2+}$ is depicted here).**

cient indicates the plots are quite linear, as they should be for a first-order reaction, and the slopes of the two concentration plots are in good agreement — the higher $Mn^{2+}$ concentration sorption resulted in a slightly higher slope. The rate constants obtained for the first-order reaction mechanism are $3.73 \times 10^{-3}$ and $3.75 \times 10^{-3}$ $s^{-1}$ for 25 and 40 $\mu M$ $[Mn^{2+}]_0$, respectively, with an averaged $k_f' = 3.74 \times 10^{-3} \pm 0.1 \times 10^{-4}$ $s^{-1}$. In addition to the $k_f'$ values being similar, the semilog plot should also yield an intercept value equal to the log $[Mn^{2+}]_0$; indeed, the intercept values are in close agreement with the known $[Mn^{2+}]_0$: 24 and 41 $\mu M$. Consequently, Eq. [7] appears to be valid for the experimental conditions invoked here.

The measured $k_f'$ was then used in combination with Eq. [6] and the known reaction parameters to calculate $k_r'$; the calculated $k_r'$ was $3.04 \times 10^{-4}$ $s^{-1}$. After determining the $k_f'$ and $k_r'$, one can predict the time dependence of $Mn^{2+}$ sorption, and for further validation of the rate constants compare the calculated values with those measured experimentally. Rearranging Eq. [4] allows the time dependence of $Mn^{2+}$ sorption to be predicted:

$$[Mn^{2+}]_t = [Mn^{2+}]_o\{k_r' + k_f' \exp -(k_f' + k_r')t/k_f' + k_r'\} \quad [10]$$

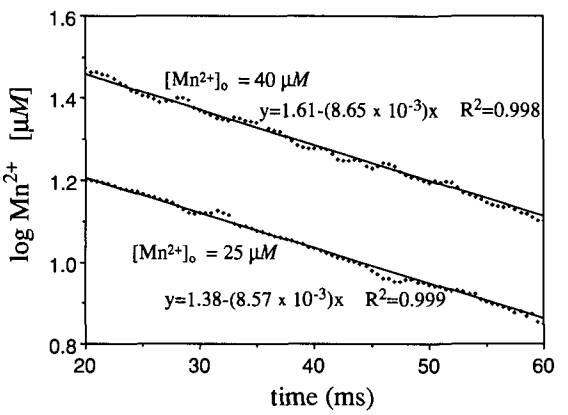


**Fig. 5. Initial reaction rates depicting the first-order dependence of $Mn^{2+}$ sorption as a function of time for initial $Mn^{2+}$ concentrations of 25 and 40 $\mu M$.**

Figure 6 illustrates the measured and predicted time dependence of $Mn^{2+}$ sorption on $\delta$-$MnO_2$. The predicted trends of $Mn^{2+}$ sorption were in good agreement with those measured, validating the accuracy of the forward and reverse rate constants.

The validation of reaction [7] as a first-order elementary reaction indicates that chemical kinetics were measured; thus, transport phenomena were not rate limiting. If diffusion processes were influencing the reaction rate, or if an incorrect reaction order was assumed, then a deviation from linearity in the semilog plot depicted in Fig. 4 would occur (the reaction would not conform solely to a first-order dependence on $[Mn^{2+}]$) and there would be poor conformity between measured and predicted $Mn^{2+}$ sorption on $\delta$-$MnO_2$ with time (Bunnett, 1986).

Determining reaction mechanisms and rates are essential to understanding, predicting, and possibly controlling chemical processes. The EPR–SF kinetic technique has shown great utility in measuring rapid reaction rates in colloidal suspensions. Moreover, the results presented here indicate that the apparatus measures chemical kinetics, devoid of transport-rate-limiting phenomena. This technique is ideally suited for sorption reactions involving colloidal material, as the need for filtration is eliminated, thus allowing rapid data acquisition of reaction constituents. The rate parameters can be used to evaluate the time scale of reactions, and to ascertain reaction mechanisms. Utilizing the rapid measurements capable with this technique, one can measure reactions at sufficiently early times so as to determine $k_f$ values. With a

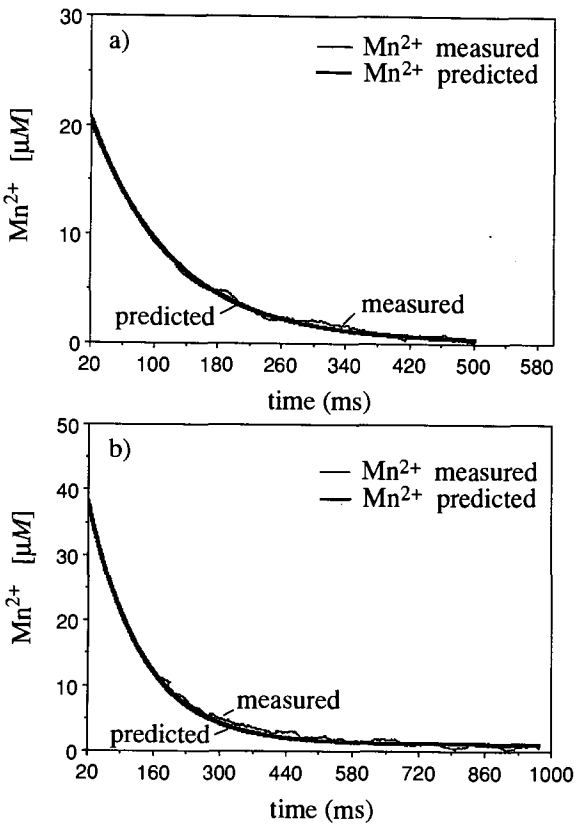


**Fig. 6. The predicted time dependence of $Mn^{2+}$ sorption on $\delta$-$MnO_2$, using the determined rate constants, compared with the measured sorption rate curve for initial $Mn^{2+}$ concentrations of: (a) 25 $\mu$M and (b) 40 $\mu$M.**

knowledge of $k_f$ values, integrated rate expressions can be used to calculate $k_r$. Furthermore, since chemical kinetics are being determined, equilibrium constants ($K_{eq}^{kin}$) can be ascertained from the ratio of $k_f/k_r$. The $K_{eq}^{kin}$ values may then be compared with equilibrium constants ($K_{eq}$) determined via traditional equilibrium approaches (Sparks, 1989).

Although the EPR–SF technique is limited to paramagnetic species, there are many agriculturally and environmentally significant species that are EPR active. The EPR–SF technique provides many advantages for studying soil chemical reactions: (i) it allows direct measurement of surface reactions involving EPR-active ions, (ii) rate constants and equilibria are thus accurately determined from direct measurements, and (iii) reaction mechanisms, necessary to determine the fate of environmental constituents, can be elucidated. Therefore, we feel that this simple yet elegant kinetic technique has great potential for studying many soil and colloidal surface reactions.

In this study, we used EPR spectroscopy only to quantitatively measure solution $Mn^{2+}$, but, depending on one's objectives, EPR spectroscopy can also be used to obtain surface information. The time necessary for a complete magnetic sweep would be prohibitive for rapid reaction measurements, thus reducing the extent of time-dependent surface information that may be obtained for such reactions (although slower reactions may be monitored continually with complete EPR spectra). Spectra can be taken prior to reaction, however, and at a steady state after reaction, giving information on surface structural alterations induced by the reaction being investigated. Such information would greatly complement many kinetic investigations.

## ACKNOWLEDGMENTS

We would like to gratefully acknowledge Battelle, Pacific Northwest Lab., for the use of their facilities, and Dr. C.C. Ainsworth for his support of this project. Partial support for this work was provided by the U.S. Department of Energy, Office of Energy Research, under Contract DE-AC06-76RLO 1830 with Battelle Memorial Institute. S.E. Fendorf appreciates the support of a University of Delaware fellowship.

## REFERENCES

Arrhenius, G., K. Cheung, S. Crane, M. Fisk, J. Frazer, J. Korkisch, T. Mellin, S. Nakao, A. Tsai, and G. Wolf. 1979. Counterions in marine manganates. Colloq. Int. CNRS 298:333–356.

Balistrieri, L.S., and J.W. Murray. 1982. The surface chemistry of $\delta MnO_2$ in major ion seawater. Geochim. Cosmochim. Acta 46:1041–1052.

Bleam, W.F., and M.B. McBride. 1986. The chemistry of adsorbed Cu(II) and Mn(II) in aqueous titanium dioxide suspensions. J. Colloid Interface Sci. 110:335–346.

Bunnett, J.F. 1986. Kinetics in Solution. p. 171–250. In C.F. Bernasconi (ed.) Investigations of rates and mechanisms of reactions. 4th ed. John Wiley & Sons, New York.

Clementz, D.M., T.J. Pinnavaia, and M.M. Mortland. 1973. Stereochemistry of hydrated copper(II) ions on the interlamellar surfaces of layer silicates. An electron spin resonance study. J. Phys. Chem. 77:196–200.

Drago, R.S. 1977. Physical methods in chemistry. Saunders College Pub., Orlando, FL.

Dzombak, D.A., and M.M. Morel. 1990. Surface complexation modeling. John Wiley & Sons, New York.

Fendorf, S.E., and R.J. Zasoski. 1992. Chromium(III) oxidation by $\delta$-$MnO_2$: I. Characterization. Environ. Sci. Technol. 26:79–85.

Hayes, K.M., and J.O. Leckie. 1986. Mechanism of lead ion adsorption at the goethite-water interface. p. 114–141. *In* J.A. Davis and K.M. Hayes (ed.) Geochemical processes at mineral surfaces Am. Chem. Soc., Washington, DC.

Hiemstra, T., W.H. Van Riemsdijk, and G.H. Bolt. 1989a. Multisite proton adsorption modeling at the solid/solution interface of (hydr)oxides: A new approach: I. Model description and evaluation of intrinsic reaction constants. J. Colloid Interface Sci. 133:91–104.

Hiemstra, T., J.C.M. De Wit, and W.H. Van Riemsdijk. 1989b. Multisite proton adsorption modeling at the solid/solution interface of (hydr)oxides. A new approach: II. Application to various important (hydr) oxides. J. Colloid Interface Sci. 133:105–117.

Ikeda, T., M. Sasaki, and T. Yasunaga. 1983. Kinetic studies of ion exchange of alkylammonium ion for sodium ion in aqueous suspensions of zeolite 4A using the pressure-jump method. J. Phys. Chem. 87:745–749.

Ikeda, T., J. Nakahara, M. Sasaki,and T. Yasunaga. 1984. Kinetic behavior of alkali metal ion on zeolite 4A surface using the stopped-flow method. J. Colloid Interface Sci. 97:278–283.

Klimes, N., G. Lassmann, and B. Ebert. 1980. Time-resolved EPR spectroscopy. Stopped-flow EPR apparatus for biological application. J. Magn. Reson. 37:53–59.

McBride, M.B. 1982. Hydrolysis and dehydration reactions of exchangeable $Cu^{2+}$ on hectorite. Clays Clay Miner. 30:200–206.

McBride, M.B. 1987. Adsorption and oxidation of phenolic compounds by iron and manganese oxides. Soil Sci. Soc. Am. J. 51:1466–1472.

McBride, M.B. 1989. Oxidation of dihydroxybenzenes in aerated aqueous suspensions of birnessite. Clays Clay Miner. 37:341–347.

Morgan, J.J., and W. Stumm. 1964. Colloid-chemical properties of manganese dioxide. J. Colloid Sci. 19:347–359.

Potter, R.M., and G.R. Rossman. 1979. The tetravalent manganese oxides: identification, hydration, and structural relationships by infrared spectroscopy. Am. Mineral. 64:1199–1218.

Sparks, D.L. 1989. Kinetics of soil chemical processes. Academic Press, New York.

Stach, J., R. Kirmse, W. Dietzsch, G. Lassmann, V.K. Belyaeva,and I.N. Marov. 1985. Ligand exchange reactions between copper(II)- and nickel(II)-chelates of different sulfur- and selenium-containing ligands: VI[1]. Kinetics of ligand exchange reactions studied by stopped-flow ESR. Inorg. Chim. Acta 96:55–59.

Zhang, P.C., and D.L. Sparks. 1990. Kinetics of selenate and selenite adsorption/desorption at the goethite/water interface. Environ. Sci. Technol. 24:1848—1856.